IEEE Access
Multidisciplinary | Rapid Review | Open Access Journal

Received May 12, 2019, accepted June 9, 2019, date of publication June 24, 2019, date of current version August 19, 2019.

Digital Object Identifier 10.1109/ACCESS.2019.2924709

A Method for Hot Spot Temperature Prediction of a 10 kV Oil-Immersed Transformer

YONGQING DENG[1], JIANGJUN RUAN[1], (Member, IEEE), YU QUAN[2], RUOHAN GONG[3], DAOCHUN HUANG[1], (Senior Member, IEEE), CIHAN DUAN[1], AND YIMING XIE[1], (Student Member, IEEE)

[1]School of Electrical Engineering and Automation, Wuhan University, Wuhan 430072, China
[2]Wuhan Power Supply Company, State Grid Hubei Electric Power Company, Wuhan 430050, China
[3]Univ. Lille, Arts et Metiers Paris Tech, Centrale Lille, HEI, EA 2697-L2EP-Laboratoire d'Electrotechnique et d'Electronique de Puissance, F-59000 Lille, France

Corresponding authors: Ruohan Gong (rhgong@whu.edu.cn) and Daochun Huang (huangdc99@163.com)

ABSTRACT This paper proposed a prediction method to predict a 10-kV oil-immersed transformer hot spot temperature (HST). A set of feature temperature points on the transformer iron shell is proposed based on fluid-thermal field calculation. These feature points, as well as transformer load rate, are taken as the input parameters of a machine learning model established by support vector regression (SVR), thus to describe their relationships with the HST. This model is trained by nine samples selected by $L_9(3^4)$ orthogonal array and applied to predict the HST of 20 test samples. The training samples are all obtained by simulation, and the test samples have consisted of simulation and transformer temperature rise test results. With effective parameter optimization of the SVR model, the predicted results agree well with the experimental and simulation data, the mean absolute percentage error (MAPE) is 1.55%, and the maximum temperature difference is less than 3 °C. The results validated the validity and the generalization performance of the prediction model.

INDEX TERMS Hot spot temperature, oil-immersed transformer, support vector regression, multi-physical field analysis.

I. INTRODUCTION

Hot spot temperature (HST) is defined as the maximum temperature point of the transformer's winding, and the deterioration of transformer oil-paper insulation is significantly affected by the HST. It is widely accepted that the ageing rate of paper insulation doubles each 6 K rise above the rated HST 371 K (98 °C) [1]. Therefore, accurate prediction of transformer's HST is of great significance.

There are many ways to detect HST. Optical fiber temperature sensors can be installed inside the transformer to measure the HST directly [2]–[4], however, due to the high cost of the optical fiber instrument, it cannot fit the demand of large-scale application, and it cannot be applied to the in-service transformer. Besides, because of the uncertainty of the specific hot spot location, it is hard to get the accurate temperature of the hot spot. Considering the analogy between electrical and heat-transfer phenomena, many classical thermal circuits are proposed to calculated the temperature of hot spot [5]–[7]. Based on thermal circuit, corresponding empirical formula is also proposed to detect HST in IEC and IEEE standards [7], [8]. However, the key parameters such as heat capacity and thermal resistance in the thermal circuit is difficult to obtain.

With the development of numerical calculation, the electromagnetic-fluid-thermal coupled method has been used in transformer HST detection. Finite element method (FEM) can be used to calculate the losses inside the windings and iron structure, and finite volume method (FVM) can be used to calculate the fluid-thermal distribution inside the transformer [9]. Numerical method can reflect the temperature and oil flow velocity distribution inside the transformer with a high accuracy. However, due to the complex structure and material nonlinearity of transformer, numerical method has a high requirement for computer performance and it often takes much computing time.

Artificial intelligence algorithms have also been applied to predict the HST inside the transformer, and they have performed a good performance. Artificial neural network was used to predict the top-oil temperature of a 22.4 MVA oil-immersed transformer [10]. The particle swarm optimizer was used to identify the thermal parameters of a simplified thermoelectric analogous thermal model in a large autotransformer (220 MVA, 400.0kV/132.0kV, ONAN/OFAF) [11]. Support vector regression machine with an improved particle

The associate editor coordinating the review of this manuscript and approving it for publication was aysegul Ucar.

swarm optimization (PSO) method has been adopted to establish a model for the prediction of HST in a 750MVA/500kV power transformer, this model has achieved a good prediction results and it is verified by the real datasets sampled from the transformer [12]. An algorithm combining support vector regression and information granulation was proposed to detect the hot spot temperature of a 15 MVA ODAF transformer, and it outperforms a number of existing thermal model based methods, namely IEEE model, Swift's model and Susa's model [13]. Based on the support vector regression optimized by genetic algorithm (GA), the performances of three commonly used models (IEEE model, Swift's model and Susa's model) for predicting transformer top oil temperature are compared in [14].

The internal relation between the HST and the temperature on the transformer iron shell and the load rate can be viewed as a complicated multi-dimensional nonlinear relationship. Based on this view, in this paper, according to the results of coupled multi-physical field computation, a set of feature temperature points on the transformer iron shell is proposed. Taking the load rate and the feature temperature points into consideration, we developed a mathematical model based on SVR to predict the HST of the transformer. The orthogonal design method is used in this paper to choose appropriate training samples. The validity of the proposed methodology is validated by transformer temperature rise test.

II. A GENERAL DESCRIPTION OF THE PREDICTION METHOD

A. BRIEF INTRODUCTION OF SVR

SVR has a strong ability in dealing with multi-dimensional non-linear problems with relatively few samples [15]. A brief introduction of ε-SVR can be described as follows [16]–[18]:

A set of training samples S can be expressed in (1), where x_i is the ith input vector, y_i is the corresponding output vector and n is the sample size.

$$S = \{(x_1, y_1), \cdots, (x_n, y_n)\} \subset R^n \times R \tag{1}$$

A hyperplane can be applied to characterizing the relationship between $\boldsymbol{x}$ and y, namely $f(x) = \omega \cdot \boldsymbol{x} + b$, where $\omega \in R^n$ and $b \in R$.

$$|y_i - f(x_i)| \le \varepsilon, \quad i = 1, 2, \cdots, n \tag{2}$$

For any point $(\boldsymbol{x}_i, y_i)$ in the training sample set, the distance to the hyperplane d_i can be expressed as:

$$d_i = \frac{|\boldsymbol{\omega} \cdot x_i + b - y_i|}{\sqrt{1 + \|\boldsymbol{\omega}\|^2}} \le \frac{\varepsilon}{\sqrt{1 + \|\boldsymbol{\omega}\|^2}}, \quad i = 1, 2, \cdots, n \tag{3}$$

There may be several hyperplanes can satisfying the requirements of (3), the optimal hyperplane should maximize the distance between the training sample set and the hyperplane, namely:

$$\begin{cases} \min & \varphi(\boldsymbol{\omega}) = \dfrac{1}{2} \|\boldsymbol{\omega}\|^2 \\ \text{s.t.} & |\boldsymbol{\omega} \cdot x_i + b - y_i| \le \varepsilon, \quad i = 1, 2, \cdots, n \end{cases} \tag{4}$$

Slack variables ξ_i and ξ_i^* can be introduced to optimize the hyperplane:

$$\begin{cases} \min & \varphi(\boldsymbol{\omega}) = \dfrac{1}{2} \|\boldsymbol{\omega}\|^2 + C \sum_{i=1}^{n} \left(\xi_i + \xi_i^*\right) \\ \text{s.t.} & f(x_i) - y_i \le \xi_i^* + \varepsilon \\ & y_i - f(x_i) \le \xi_i + \varepsilon \\ & \xi_i, \xi_i^* \ge 0, \quad i = 1, 2, \cdots, n \end{cases} \tag{5}$$

where C is the penalty factor, ε is the insensitive loss coefficient.

By introducing the lagrangian multipliers α_i and α_i^* and γ_i, the lagrange function of (5) is:

$$\begin{cases} L = \dfrac{1}{2}\|\boldsymbol{\omega}\|^2 + C\sum_{i=1}^{n}\left(\xi_i + \xi_i^*\right) - \sum_{i=1}^{n} \alpha_i \left[\xi_i + \varepsilon - y_i + \boldsymbol{w} \cdot \boldsymbol{x}_i + b\right] \\ \qquad - \sum_{i=1}^{n} \alpha_i^* \left[\xi_i^* + \varepsilon + y_i - \boldsymbol{w} \cdot \boldsymbol{x}_i - b\right] - \sum_{i=1}^{n} \gamma_i \left(\xi_i + \xi_i^*\right) \\ \text{s.t.} \quad \alpha_i,\ \alpha_i^*,\ \gamma_i \ge 0,\ i = 1, 2, \cdots, n \end{cases} \tag{6}$$

If the extremum of function L exists, the partial derivatives of L with respect to ω, b, ξ_i and ξ_i^* are all 0, it can be derived that:

$$\omega = \sum_{i=1}^{n} \left(\alpha_i - \alpha_i^*\right) x_i, \quad \sum_{i=1}^{n} \left(\alpha_i - \alpha_i^*\right) = 0,$$
$$C - \alpha_i - \gamma_i = 0, \quad C - \alpha_i^* - \gamma_i^* = 0,\ i = 1, 2, \cdots, n \tag{7}$$

Substituting (7) into (6), and import the kernel function to transform the training sample data from the original input space to a higher-dimensional feature space, the dual problem of ε-SVR can be deduced as:

$$\begin{cases} \max & W(\alpha, \alpha^*) = \dfrac{1}{2} \sum_{i=1}^{n} \left(\alpha_i - \alpha_i^*\right) \left(\alpha_j - \alpha_j^*\right) K(\boldsymbol{x}_i \cdot \boldsymbol{x}_j) \\ & \qquad + \sum_{i=1}^{n} \left(\alpha_i - \alpha_i^*\right) y_i - \sum_{i=1}^{n} \left(\alpha_i + \alpha_i^*\right) \varepsilon \\ \text{s.t.} & \sum_{i=1}^{n} \left(\alpha_i - \alpha_i^*\right) = 0, \quad 0 \le \alpha_i, \alpha_i^* \le C,\ i = 1, 2, \cdots, n \end{cases} \tag{8}$$

where $K(x_\mathrm{i}, x_\mathrm{j}) = \varphi(x_\mathrm{i})^T \varphi(x_\mathrm{j})$ is the kernel function.

The parameter of the radial basis function (RBF) kernel function is simple and it can effectively realize a non-linear mapping. Thus RBF kernel is selected in this paper, it can be expressed as:

$$K(\boldsymbol{x}_i, \boldsymbol{x}) = \exp(-\gamma \|\boldsymbol{x} - \boldsymbol{x}_i\|^2), \quad \gamma > 0 \tag{9}$$

By solving the above equations, the expression of the optimal hyperplane of the corresponding sample training set is:

$$f(x) = \sum_{i=1}^{n} \left(\alpha_i - \alpha_i^*\right) K(x_i, x) + b \tag{10}$$

The LIBSVM toolbox developed by Dr. Chih-Jen Lin of National Taiwan University is used in this paper to solve the regression problem [19].

B. TRANSFORMER MULTI-PHYSICAL FIELD ANALYSIS

1) ELECTROMAGNETIC FIELD

According to Maxwell equations, the governing equation of quasi-static magnetic field problem based on magnetic vector potential is shown as follows [9]:

$$\nabla \times \frac{1}{\mu}(\nabla \times \boldsymbol{A}) = \boldsymbol{J}_s - \sigma \frac{\partial \boldsymbol{A}}{\partial t} \tag{11}$$

where μ is the magnetic permeability, σ is the conductivity, A is the magnetic vector potential, and J_s is the current density vector.

2) FLUID-THERMAL FIELD

The transformer internal oil flow can be described by the mass conservation equation, momentum conservation equation and energy conservation equation [20]. To solve the thermal-fluid field coupled equations, the commercial finite volume CFD code Ansys-CFX V15.0 is used.

$$\nabla \cdot v = 0 \tag{12}$$

$$\rho \frac{Dv}{Dt} = \rho \boldsymbol{g} - \frac{\partial \boldsymbol{p}}{\partial x} + \mu \nabla^2 v \tag{13}$$

$$\rho c v \cdot \nabla T = \nabla \cdot k \nabla T + q \tag{14}$$

where, ρ is the oil density; v is the fluid velocity; g stands for the gravity acceleration; p represents the pressure; μ denotes the dynamic viscosity; k is the thermal conductivity; c is the specific heat capacity; T represents the temperature; q indicates the heat source per volume inside the transformer.

The external heat dissipation mainly depends on the heat convection along the surfaces of the transformer. Heat flux q induced by external convection can be described by (15):

$$q = hS(T - T_f) \tag{15}$$

where, q is the heat flux per unit area, W/m^2; T and T_f is the temperature of the wall and external fluids respectively; S is the surface area of the wall; h is the heat convection coefficient.

Heat convection coefficient h can be obtained from following equation [21]:

$$N_u = aR_a^b = \frac{hL}{k} \tag{16}$$

where, N_u is the Nusselt number; R_a is the Rayleigh number; a and b are constants determined by the system; L is the feature size;k is the thermal conductivity.

According to heat-transfer theory [22], [23], the Nusselt number of vertical plane Nu_{v} and horizontal plane Nu_{h} can be analyzed by the following equations:

$$Nu_v = 0.59Ra^{1/4} \tag{17}$$

$$Nu_h = 0.27Ra^{1/4} \tag{18}$$

TABLE 1. Thermodynamic parameters of the transformer oil.

Physical parameters	Fitting value
ρ (kg·m^{-3})	$1098.72\text{-}0.712T$
c(J·kg-1·K^{-1})	$807.163\text{+}3.58T$
k(W·m-1·K^{-1})	$0.1509\text{-}7.101\times10^{-5}T$
μ(Pa·S)	$0.08467\text{-}4\times10^{-4}T\text{+}5\times10^{-7}T^2$

FIGURE 1. S13-M-100 kVA/10 kV transformer.

The thermal parameter characteristics of the transformer oil are specified on Table 1, all parameters vary with the temperature to get a better simulation accuracy [24], [25].

3) ORTHOGONAL DESIGN METHOD

Since the temperatures of the training samples are obtained by coupled multi-physical field calculation, there should be a reasonable sampling method to ensure the prediction accuracy of the model and reduce simulation work simultaneously. Hence, the orthogonal design method is used in this paper to choose appropriate training samples.

Orthogonal design method is a scientific method for arranging and analyzing multi-factor tests, it was first proposed by Taguchi *et al.* [26]. Orthogonal design method is used for two purposes in experimental design, the first one is to minimize the number of tests, and the second one is to get the best results on the basis of fewer tests. By selecting samples uniformly and orderly, orthogonal design method is useful and efficient to solve experimental problems with multiple factors and levels [27].

Orthogonal arrays can be expressed as $L_a(b^c)$, where a is the total number of test runs, b is the number of levels of each factor, and c is the number of influencing factor of the tests. In this paper, the orthogonal design method is applied to select training samples used for the SVR prediction model. There are four factors including the transformer load rate, ambient temperature, wind speed and humidity. Each factor has three levels. Hence, a $L_9(3^4)$ orthogonal array is used to select training samples in this paper.

III. TRANSFORMER TEMPERATURE RISE TEST AND MULTI-PHYSICAL FIELD ANALYSIS

A. TRANSFORMER TEMPERATURE RISE TEST

In this paper, a S13-M-100 kVA/10 kV transformer is selected as the research object, the basic parameters of the transformer are shown in Table 2, and the structure of the transformer is shown in Fig. 1. The transformer temperature rise test is

TABLE 2. Basic parameters of the transformer.

Basic parameters	Value
Rated capacity	100 kVA
Voltage	10000±2×2.5%/400 V
Connection group	Dyn11
Rated frequency	50Hz
Cooling method	ONAN
Number of phases	Three phases

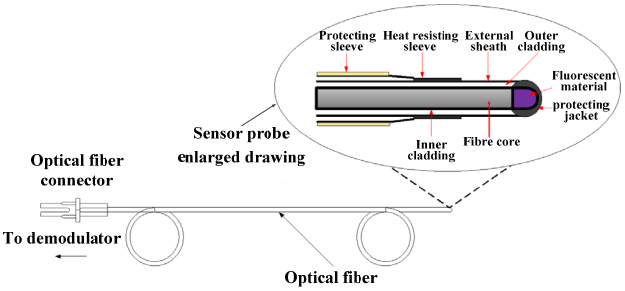

FIGURE 2. Optical fiber temperature sensor.

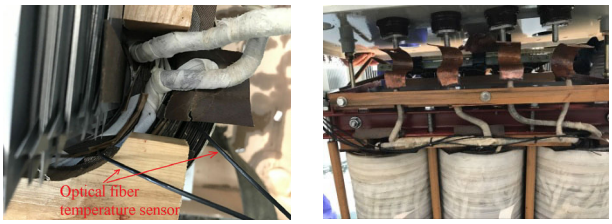

FIGURE 3. Optical fiber temperature sensors arrangement in temperature rise test.

conducted by short circuit method, during the temperature rise test, thermal resistance temperature sensors are used to measure the temperature rise on the transformer iron shell, and optical fiber temperature sensors are used to measure the temperature in the winding of the transformer to validate the feasibility and accuracy of the proposed 3-D coupled magneto-fluid-thermal simulation method.

The FTM-6CH-H220 optical fiber temperature sensor used in the test has a temperature measurement range from −40 °C to 200 °C. Two optical fiber temperature sensors are installed in each phase low voltage winding and high voltage winding respectively, the structure of the optical fiber is shown in Fig. 2, and the installation position of the optical fiber is shown in Fig. 3. The installation position of the thermal resistance temperature sensors on transformer iron shell is shown in Fig. 4.

B. TRANSFORMER MULTI-PHYSICAL FIELD ANALYSIS

Under normal operating conditions, the total transformer losses including iron loss, winding copper loss and stray loss. Before the temperature rise test, the no-load loss and load loss of the transformer are obtained through no-load test and load test of the transformer under rated load condition, and

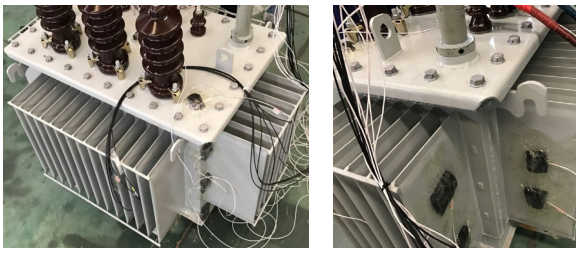

FIGURE 4. Thermal resistance temperature sensors arrangement in temperature rise test.

the value is 149.2W and 1517.3W respectively. It can be considered that the value of iron loss and no-load loss of the transformer are basically the same, and load losses are mainly consists of transformer winding loss and stray loss on the transformer iron shell. The stray loss on transformer iron shell is calculated by finite element method (FEM), and the specific value is 11.9 W, thus the loss on transformer windings is 1505.4W. Therefore, the winding loss accounts for the majority of the total loss, stray loss on transformer iron shell accounts for a small part.

The temperature rise test of the transformer is carried out by the short circuit method, during the test, the total losses loaded on the transformer is the sum of the load loss and no-load loss of the transformer, and the total loss value under rated condition is 1666.5W. As the iron loss on transformer core is very small in the short circuit temperature rise test method, and the calculated stray loss on the transformer iron shell takes a very small proportion of the total loss, less than 0.75%, thus it can be considered that almost all the losses in the temperature rise test are loaded on transformer windings. Based on this, all heat sources are loaded on the transformer windings in the thermal-fluid field analysis.

The formula for calculating transformer losses under different load rate is as follows:

$$P = n^2 \times P_l + P_w \tag{19}$$

where n is the transformer load rate; P_l is the load loss at rated load rate; P_{w} is the no-load loss at rated load rate.

A three-dimensional transformer simulation model including high and low voltage windings, iron core, oil tank and radiator structure is established in the analysis. In order to obtain grid with a high quality, hexahedral mesh mapping partition is used to partition transformer windings, and tetrahedral mesh is used to partition irregular parts of the transformer, such as the fluid domain of transformer oil, the iron core inside the transformer, the oil tank and radiator shell. The meshes of the model are shown in Fig. 5, and the total mesh number of the model is 2.53 million.

The measured and calculated temperature comparison under different load rate is shown in Table 3, and the calculated temperature distribution of the transformer at ratio 1.0 is shown in Fig. 6. The maximum error between calculated and experimental results is not more than 3 °C.

TABLE 3. Temperature comparison of measured and calculated values under different load rates.

Load rate		Typical temperature measure point (℃)				
		Winding hot spot	Top center of the oil tank	2/3 height of the oil tank wide side	Bottom center of the oil tank	Ambient temperature
0.7	Measured data	53.2	27.6	27.9	15.1	9.0
	Calculated result	51.1	28.5	27.0	15.2	
0.8	Measured data	60.1	32.9	32.9	17.8	6.5
	Calculated result	59.7	33.9	33.3	19.1	
0.9	Measured data	64.7	34.5	34.9	17.4	5.0
	Calculated result	64.9	35.6	35.3	19.4	
1.0	Measured data	74.6	42.4	43.2	22.7	7.5
	Calculated result	72.6	42.4	43.1	24.7	
1.1	Measured data	83.4	48.1	49.0	25.4	7.0
	Calculated result	82.7	47.7	49.6	28.2	
1.2	Measured data	93.2	54.5	56.2	29.3	8.0
	Calculated result	93.5	53.8	57.0	30.0	

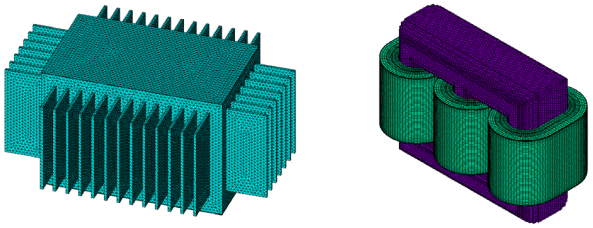

(a) (b)

FIGURE 5. Model mesh generation: (a) Transformer iron shell, (b) Iron core and windings.

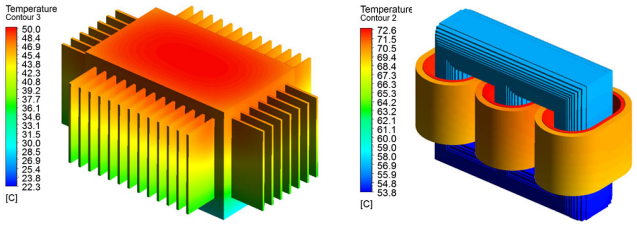

(a) (b)

FIGURE 6. Temperature distribution of the transformer: (a) Transformer iron shell, (b) Iron core and windings.

C. FEATURE TEMPERATURE POINTS ON TRANSFORMER IRON SHELL

Transformer oil stream line reflects the flow path of transformer oil. According to the calculation results of transformer coupled multi-physical field analysis, main stream lines flowing through transformer oil tank and windings are extracted, and they are shown in Fig. 7. The main stream lines flowing out from the hot area of windings can be divided into two categories, one is cooled by the wide side radiator of the shell and then flow into the bottom of the tank, the other is cooled by the narrow side radiator of the shell and then flow into the bottom of the tank. Based on this phenomenon, six temperature points of transformer iron shell are selected as the feature temperature points, these points are shown in Fig. 8, and the specific positions are shown in Table 4.

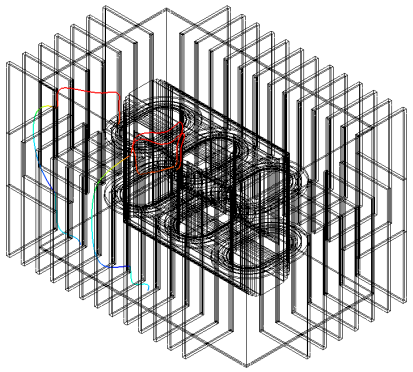

FIGURE 7. Main stream line in S13-M-100 kVA/10 kV transformer.

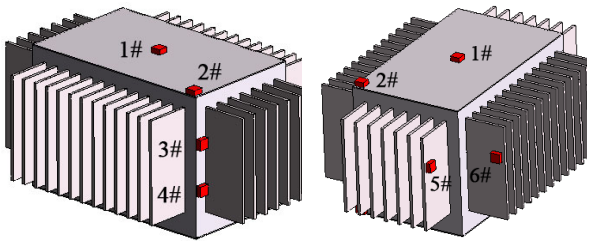

FIGURE 8. Feature temperature points on transformer iron shell.

IV. HOT SPOT TEMPERATURE PREDICTION

A. SELECTION OF TRAINING AND TEST SAMPLES

The method proposed in this paper for HST prediction is based on coupled multi-physical field analysis and SVR. The input in the SVR model is a set of feature temperature points on the transformer iron shell and transformer load rate, the output of the model is the HST inside the transformer. Once the relationship is established, we only need to monitor the transformer load rate and temperature on the feature temperature points to get the HST of the transformer.

The relationship between the output and input is obtained by training sample learning. Therefore, the selection of training samples directly affects the accuracy of the algorithm. Transformer load rate, ambient temperature, wind speed and

TABLE 4. The locations of feature temperature points.

No.	Locations
1#	top center of the oil tank
2#	top edge corner of the oil tank
3#	2/3 height of the oil tank outer edge corner
4#	1/3 height of the oil tank outer edge corner
5#	2/3 height of the narrow edge radiator
6#	2/3 height of the wide edge radiator

TABLE 5. Four factors and three levels orthogonal table parameters.

Level \ Factor	Load rate	Wind speed (m/s)	Ambient temperature (°C)	Humidity (%)
1	0.6	0	0	20
2	1.0	2	10	40
3	1.3	4	20	60

TABLE 6. Four factors and three levels orthogonal table (training samples).

No.	Load rate	Wind speed (m/s)	Ambient temperature (°C)	Humidity (%)
1	0.6	0	20	20
2	0.6	2	10	40
3	0.6	4	0	60
4	1.0	0	10	60
5	1.0	2	0	20
6	1.0	4	20	40
7	1.3	0	0	40
8	1.3	2	20	60
9	1.3	4	10	20

humidity can influence the temperature distribution on transformer iron shell significantly. In order to improve the generalization performance of the prediction model, the training samples should contain as many transformer operating conditions as possible. The proposed $L_9(3^4)$ orthogonal array is shown in Table 5, and specific training samples are shown in Table 6.

Test samples are used to verify the universality and extensibility of the model in other situations. The test samples selected in this paper are shown in Table 7, in which samples 1 to 12 are actual transformer temperature rise test results, and samples 13 to 20 are the simulation results.

B. MODEL TRAINING AND PARAMETER OPTIMIZATION

Through the analysis of SVR model with RBF kernel, we can see that penalty coefficient C and kernel function parameter γ determine the model generalization ability. In this paper, based on the idea of K-fold cross-validation, the grid search (GS) method is used to find the optimal parameters of C and γ. As for the K-fold cross-validation, the original data is divided into K groups, among which K-1 groups are used as training samples and the remaining one group is used as the test sample for each testing. In this paper, for the 9 training samples, K is set as 9. This procedure was carried out repeatedly for 9 times. The average value of the mean square error

TABLE 7. Test samples.

No.	Load rate	Wind speed (m/s)	Ambient temperature (°C)	Humidity (%)
1	0.8	0	6.5	50
2	1	0	7.5	55
3	1.1	0	7	60
4	1.2	0	8	60
5	0.9	0	5	48
6	0.7	0	9	46
7	0.8	2	5	50
8	0.7	1	7.5	30
9	1.2	3	7	26
10	1.1	2	5.5	26
11	0.9	1	10.5	30
12	1	3	6.5	30
13	0.64	0.5	2	18
14	0.75	1.2	5	36
15	0.83	0.7	7	44
16	0.95	1	7.5	18
17	1.06	1.8	3	28
18	1.08	2.4	11	38
19	1.12	1.5	5	40
20	1.22	2.8	7	16

(MSE) for the 9 trials was taken as the performance indicator of the SVR model.

The features in the model include the transformer load rate and the temperatures on the feature temperature points. In order to eliminate the effects of different orders of magnitude and dimensions, these features are normalized within the range [0, 1] by the following formula [28]:

$$x_i' = \frac{x_i - x_{\min}}{x_{\max} - x_{\min}} \tag{20}$$

where x_i is the ith feature, $x_{\min}$ and $x_{\max}$ are its minimum and maximum values and x_i' is its normalized value.

C. ERROR ANALYSIS METHOD

Error analysis is one of the important steps to test the HST prediction model of oil-immersed transformer. Through error analysis, the advantages and disadvantages of the model algorithm can be evaluated scientifically, and the reasonable application of the model can be guided.

In this paper, four error indexes are used to compare the predicted and experimental values [29], namely:

1) Sum of squared error, SSE

$$e_{\text{SSE}} = \sum_{i=1}^{N} (A_i - P_i)^2 \tag{21}$$

2) Root mean squared error, RMSE

$$e_{\text{RMSE}} = \sqrt{\frac{1}{N} \sum_{i=1}^{N} (A_i - P_i)^2} \tag{22}$$

3) Mean absolute percentage error, MAPE

$$e_{\text{MAPE}} = \frac{1}{N} \sum_{i=1}^{N} \left| \frac{A_i - P_i}{A_i} \right| \tag{23}$$

TABLE 8. Parameter optimization results of GS algorithm.

parameters	results
C	11585.24
γ	1.31×10^{-4}

TABLE 9. Prediction of test results using GS-SVR and empirical formula.

NO.	HST measured value /℃	GS-SVR		Empirical formula	
		Predicted value /℃	Error /℃	Calculated value /℃	Error /℃
1	60.1	58.38	1.72	55.20	4.90
2	74.6	73.59	1.01	74.50	0.10
3	83.6	82.87	0.73	84.10	-0.50
4	93.2	92.97	0.23	95.79	-2.59
5	64.7	63.77	0.93	62.52	2.18
6	51.8	50.20	1.60	49.56	2.24
7	50.5	49.67	0.83	55.20	-4.70
8	48.8	47.57	1.23	49.56	-0.76
9	77.2	75.16	2.04	95.79	-18.59
10	70.6	68.92	1.68	84.10	-13.50
11	61.8	61.77	0.03	62.52	-0.72
12	62.4	61.30	1.10	74.50	-12.10

4) Mean square percentage error, MSPE

$$e_{\mathrm{MSPE}} = \frac{1}{N}\sqrt{\sum_{i=1}^{N}\left(\frac{A_i - P_i}{A_i}\right)^2} \tag{24}$$

where A_i is the experimental HST value, P_i is the predicted HST value, N is the sample size.

D. RESULTS AND DISCUSSION

The optimization results of kernel function parameters and penalty coefficient of corresponding training samples under GS algorithm are shown in Table 8.

Based on the optimal parameters obtained by the training samples, the GS optimized SVR model is used to predict the HST in the test samples. As the test samples is consisted of actual transformer temperature rise results and simulation results, the predicted values are compared with HST measured value and simulation value respectively, which are shown in Table 9 and Table 10.

In order to verify the superiority of the HST prediction method for S13-M-100 kVA/10 kV oil-immersed transformer, in this section, the recommended empirical formula by IEC are used to calculate the steady-state HST of the test samples, the empirical formula can be described as follows [1]:

When the HST rises:

$$\theta_h(t) = \theta_a + \Delta\theta_{oi} + \left\{\Delta\theta_{or}\times\left[\frac{1+RK^2}{1+R}\right]^x - \Delta\theta_{oi}\right\}\times f_1(t) + \Delta\theta_{hi} + \left\{Hg_rK^y - \Delta\theta_{hi}\right\}\times f_2(t) \tag{25}$$

When the HST falls:

$$\theta_h(t) = \theta_a + \Delta\theta_{or}\times\left[\frac{1+RK^2}{1+R}\right]^x + \left\{\Delta\theta_{oi} - \Delta\theta_{or}\times\left[\frac{1+RK^2}{1+R}\right]^x\right\}\times f_3(t) + Hg_rK^y \tag{26}$$

TABLE 10. Prediction of simulation results using GS-SVR and empirical formula.

NO.	HST simulation value /℃	GS-SVR		Empirical formula	
		Predicted value /℃	Error /℃	Calculated value /℃	Error /℃
13	39.62	40.35	-0.73	38.02	1.60
14	47.66	47.93	-0.27	49.54	-1.88
15	54.96	55.18	-0.22	58.27	-3.31
16	63.11	62.99	0.12	69.68	-6.57
17	64.93	64.35	0.58	75.99	-11.06
18	71.56	72.21	-0.65	86.03	-14.47
19	71.55	71.91	-0.36	84.19	-12.64
20	78.06	79.66	-1.60	97.00	-18.94

TABLE 11. Error indicators of GS-SVR and empirical formula.

Indicators \ Method	GS-SVR	Empirical formula
SSE	31.98	1577.26
RMSE	1.26	8.88
MAPE	1.55×10^{-2}	9.92×10^{-2}
MSPE	4.32×10^{-3}	2.81×10^{-2}

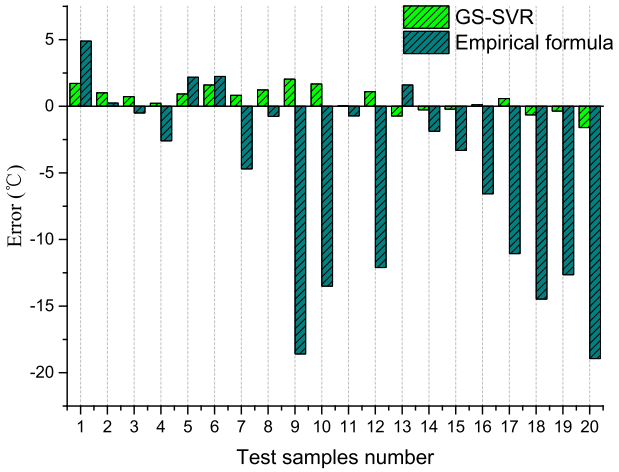

FIGURE 9. Prediction results comparison of GS-SVR and empirical formula.

where θ_a is the ambient temperature, $\Delta\theta_{oi}$ is the transformer top oil initial temperature rise, θ_{or} is the top oil temperature (TOT) rise under rated loss, $\Delta\theta_{hi}$ is the initial gradient of HST to TOT, R is the ratio of load loss to no-load loss under rated current, K is the load rate, x is the transformer oil index, y is the transformer winding index, H is the HST index, g_r is the gradient of winding average temperature to oil average temperature at rated current, $f_1(t)$, $f_2(t)$ and $f_3(t)$ are the exponential function of time.

The comparison results of GS-SVR model and empirical formula are also shown in Table 9 and Table 10.

The winding HST errors calculated by GS-SVR model and empirical formula are shown in Fig. 9, and the error indicators are shown in Table 11.

It can be seen that GS-SVR has achieved good results in the prediction of test samples, and the maximum temperature

difference is less than 3 °C. The temperature difference calculated by empirical formula is much larger than GS-SVR, and in some cases it is even more than 15 °C. In fact, the wind speed and humidity can directly affect the heat exchange efficiency between the transformer iron oil tank and the environment. The greater the wind speed, the better the convective heat transfer effect between the air and transformer iron shell. Therefore, the transformer will have a lower hot spot temperature at a higher external wind speed. When the humidity is high in the external environment, the thermal conductivity of the air will become larger, thus it can also enhances the convective heat transfer effect between the air and transformer iron shell. Ultimately, the transformer will also have a lower hot spot temperature. As for the empirical formula for calculating transformer hot-spot temperature recommended in IEC standard, the hot spot temperature of the transformer is mainly determined by ambient temperature and load rate, the effects of ambient wind speed and humidity cannot be considered. Therefore, the hot spot temperature calculation error of the empirical formula is large when the ambient wind speed is high.

V. CONCLUSIONS

Based on the feature temperature points and SVR, this paper has proposed a novel mathematical model to predict the hot spot temperature of a 10 kV oil-immersed distribution transformer. The model is trained by nine samples randomly selected according to the orthogonal design method. The trained SVR model is able to predict the HST of 20 test samples including 12 of test results and 8 of simulation results, the mean absolute percentage error of the 20 test samples is only 1.55 %. The SVR model proposed in this paper outperforms the empirical formula recommended in IEC standard.

ACKNOWLEDGMENT

The authors would like to appreciate the test support provided by China Shandong Huineng electric Company Ltd.

REFERENCES

[1] *Power Transformers—Part 7: Loading Guide for Oil-Immersed Power Transformers*, document IEC 60076-7, 2005.

[2] J. Teunissen, R. Merte, and D. Peier, "Stability of fiber Bragg grating sensors for integration into high-voltage transformers for online monitoring," in *15th Opt. Fiber Sensors Conf. Tech. Dig.*, Portland, OR, USA, May 2002, pp. 541–544.

[3] P. Hou, L. Zheng, L. Wang, and Y. Wang, "Novel method for improving the space resolution of distributed optical fiber temperature sensing system using decoupling technique," *Proc. SPIE*, vol. 4220, pp. 176–180, Oct. 2000.

[4] M. Kim, J.-H. Lee, J.-Y. Koo, and M. Song, "A study on internal temperature monitoring system for power transformer using pptical fiber Bragg grating sensors," in *Proc. Int. Symp. Elect. Insulating Mater. (ISEIM)*, Mie, Japan, Sep. 2002, pp. 163–166.

[5] G. Swift, T. S. Molinski, and W. Lehn, "A fundamental approach to transformer thermal modeling. I. Theory and equivalent circuit," *IEEE Trans. Power Del.*, vol. 16, no. 2, pp. 171–175, Apr. 2001.

[6] D. Susa, J. Palola, M. Lehtonen, and M. Hyvarinen, "Temperature rises in an OFAF transformer at OFAN cooling mode in service," *IEEE Trans. Power Del.*, vol. 20, no. 4, pp. 2517–2525, Oct. 2005.

[7] *Loading Guide for Oil-Immersed Power Transformers*, document IEC 354, 1995.

[8] *IEEE Guide for Loading Mineral-Oil-Immersed Transformers and Step-Voltage Regulators*, IEEE Standards C57.91, 2011.

[9] C. Liao, J. Ruan, C. Liu, W. Wen, and Z. Du, "3-D coupled electromagnetic-fluid-thermal analysis of oil-immersed triangular wound core transformer," *IEEE Trans. Magn.*, vol. 50, no. 11, pp. 1–4, Nov. 2014.

[10] Q. He, J. Si, and D. J. Tylavsky, "Prediction of top-oil temperature for transformers using neural networks," *IEEE Trans. Power Del.*, vol. 15, no. 4, pp. 1205–1211, Oct. 2000.

[11] W. H. Tang, S. He, E. Prempain, Q. H. Wu, and J. Fitch, "A particle swarm optimiser with passive congregation approach to thermal modelling for power transformers," in *Proc. IEEE Congr. Evol. Comput.*, vol. 3, Sep. 2005, pp. 2745–2751.

[12] W. Chen, X. Su, X. Chen, Q. Zhou, and H. Xiao, "Combination of support vector regression with particle swarm optimization for hot-spot temperature prediction of oil-immersed power transformer," *Przeglad Elektrotechniczny*, vol. 88, no. 8, pp. 172–176, Jan. 2012.

[13] Y. Cui, H. Ma, and T. Saha, "Transformer hot spot temperature prediction using a hybrid algorithm of support vector regression and information granulation," in *Proc. IEEE PES Asia–Pacific Power Energy Eng. Conf. (APPEEC)*, Brisbane, QLD, Australia, Nov. 2015, pp. 1–5.

[14] T. Qian, W. H. Tang, and W. J. Jin, "Comparisons of transformer top-oil temperature calculation models using support vector regression optimized by genetic algorithm," in *Proc. 24th Int. Conf. Electr. Distrib.*, 2017, pp. 12–15.

[15] V. N. Vapnik, *The Nature of Statistical Learning Theory*. New York, NY, USA: Springer-Verlag, 2000.

[16] Z. H. Zhou, *Machine Learning*. Beijing, China: Tsinghua Univ. Press, 2016.

[17] R. J. Liao, H. Zheng, S. Grzybowski, and L. Yang, "Particle swarm optimization-least squares support vector regression based forecasting model on dissolved gases in oil-filled power transformers," *Electr. Power Syst. Res.*, vol. 81, no. 12, pp. 2074–2080, Dec. 2011.

[18] S. Li, H. Fang, and X. Liu, "Parameter optimization of support vector regression based on sine cosine algorithm," *Expert Syst. Appl.*, vol. 91, pp. 63–77, Jan. 2018.

[19] C. C. Chang and C. J. Lin, "LIBSVM: A library for support vector machines," *ACM Trans. Intell. Syst. Technol.*, vol. 2, no. 3, pp. 1–27, 2011.

[20] R. Gong, J. Ruan, J. Chen, Y. Quan, J. Wang, and C. Duan,"Analysis and experiment of hot-spot temperature rise of 110 kV three-phase three-limb transformer," *Energies*, vol. 10, no. 8, pp. 1079–1091, Jul. 2017.

[21] R. Gong, J. Ruan, J. Chen, Y. Quan, J. Wang, and S. Jin, "A 3-D coupled magneto-fluid-thermal analysis of a 220 kV three-phase three-limb transformer under DC bias," *Energies*, vol. 10, no. 4, pp. 422–431, Mar. 2017.

[22] Y. A. Çengel, *Introduction to Thermodynamics and Heat Transfer*, New York, NY, USA: McGraw-Hill, 2008.

[23] J. Ruan, Y. Wu, P. Li, M. Long, and Y. Gong, "Optimum methods of thermal-fluid numerical simulation for switchgear," *IEEE Access*, vol. 7, pp. 32735–32744, 2019.

[24] N. El Wakil, N.-C. Chereches, and J. Padet, "Numerical study of heat transfer and fluid flow in a power transformer," *Int. J. Therm. Sci.*, vol. 45, no. 6, pp. 615–626, 2006.

[25] Y. Zhang, S. Ho, and W. Fu, "Numerical study on natural convective heat transfer of nanofluids in disc-type transformer windings," *IEEE Access*, vol. 7, pp. 51267–51275, 2019.

[26] G. Taguchi, S. Chowdhury, and Y. Wu, *Taguchi's Quality Engineering Handbook*. Hoboken, NJ, USA: Wiley, 2004, pp. 584–596.

[27] Z. Qiu, J. Ruan, D. Huang, M. Wei, L. Tang, C. Huang, W. Xu, and S. Shu, "Hybrid prediction of the power frequency breakdown voltage of short air gaps based on orthogonal design and support vector machine," *IEEE Trans. Dielectr. Elect. Insul.*, vol. 23, no. 2, pp. 795–805, Apr. 2016.

[28] Z. Qiu, J. Ruan, W. Xu, X. Wang, and D. Huang, "Electrostatic field features on the shortest interelectrode path and a SVR model for breakdown voltage prediction of rod–plane air gaps," *IET Sci., Meas. Technol.*, vol. 12, no. 7, pp. 886–892, Oct. 2018.

[29] Z. Qiu, J. Ruan, D. Huang, X. Li, F. Wang, and W. Yao, "Study on glaze electrical erosion characteristics of porcelain post insulator by using inclined plane and graphite-layer-based method," *IEEE Trans. Dielectr. Electr. Insul.*, vol. 22, no. 6, pp. 3385–3394, Dec. 2015.

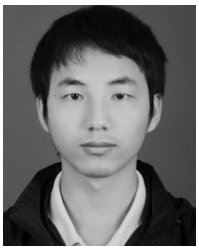

YONGQING DENG was born in Jiangxi, China, in 1992. He received the B.S. degree in electrical engineering and automation from the School of Electrical Engineering, Wuhan University, Wuhan, China, in 2016, where he is currently pursuing the Ph.D. degree with the School of Electrical Engineering and Automation. His main research interests include high voltage and insulation technology, numerical analysis, and engineering application of electromagnetic field.

JIANGJUN RUAN (M'03) was born in Zhejiang, China, in 1968. He received the B.S. and Ph.D. degrees in electric machine engineering from the Huazhong University of Science and Technology, Wuhan, China, in 1990 and 1995, respectively. He was a Postdoctoral Researcher with the Wuhan University of Hydraulic and Electric Engineering, Wuhan, in 1998. He is currently a Professor with the School of Electrical Engineering and Automation, Wuhan University. His research interests include electromagnetic field numerical simulation, high voltage, and insulation technology.

YU QUAN was born in Jiangxi, China, in 1995. She received the master's degree from Wuhan University, in 2019. She is currently with the Wuhan Power Supply Company of Hubei. Her research interests include multi-physical field simulation, transformer condition assessment, high voltage, and insulation technology. Her main research interest includes the application of artificial intelligence algorithm in transformer hot spot prediction.

RUOHAN GONG was born in Jiangxi, China, in 1991. He received the B.Eng. degree in electronic technology, in 2012, and the Ph.D. degree in electrical engineering from Wuhan University, Wuhan, China, in 2018. He holds a postdoctoral position with the University of Lille. His current research interests include multi-physical analysis and deep learning.

DAOCHUN HUANG (S'08–M'10–SM'18) was born in Heilongjiang, China, in 1976. He received the B.S. degree in electrical engineering and its automation, and the Ph.D. degree in high voltage and insulation technology from the School of Electrical Engineering, Wuhan University, Wuhan, China, in 2003 and 2009, respectively. He is currently a Professor with the School of Electrical Engineering and Automation, Wuhan University. His research interests include external insulation of transmission and transformation equipment, high voltage apparatus, and numerical analysis of electromagnetic field and its applications in engineering. He is a member of the IEEE Dielectrics and Electrical Insulation Society and the International Council on Large Electric Systems (CIGRE).

CIHAN DUAN was born in Hubei, China, in 1995. He is currently pursuing the master's degree with the School of Electrical Engineering and Automation, Wuhan University. His research interest includes transformer temperature-fluid field coupling simulation and its engineering application.

YIMING XIE (S'18) was born in Anhui, China, in 1993. He is currently pursuing the Ph.D. degree in high voltage and insulation technology with the School of Electrical Engineering and Automation, Wuhan University. His research interests include multi-physical field simulation, condition monitoring of electric device, high voltage, and insulation technology.